Hindawi Publishing Corporation
International Journal of Photoenergy
Volume 2014, Article ID 563879, 14 pages
http://dx.doi.org/10.1155/2014/563879

Review Article

One-Dimensional Nanostructured TiO_2 for Photocatalytic Degradation of Organic Pollutants in Wastewater

Ting Feng,[1] Gen Sheng Feng,[1] Lei Yan,[2] and Jia Hong Pan[3]

[1] *School of Metallurgical and Ecological Engineering, University of Science and Technology Beijing, Beijing 100083, China*
[2] *College of Materials, Optoelectronics and Physics, Xiangtan University, Xiangtan, Hunan 411105, China*
[3] *Department of Materials Science and Engineering, NUSNNI-NanoCore, National University of Singapore, Singapore 117576*

Correspondence should be addressed to Ting Feng; fengting@ustb.edu.cn and Lei Yan; yanlei@xtu.edu.cn

Received 4 April 2014; Revised 12 June 2014; Accepted 23 June 2014; Published 5 August 2014

Academic Editor: Xiwang Zhang

The present paper reviews the progress in the synthesis of one-dimensional (1D) TiO_2 nanostructures and their environmental applications in the removal of organic pollutants. According to the shape, 1D TiO_2 nanostructures can be divided into nanorods, nanotubes, nanowires/nanofibers, and nanobelts. Each of them can be synthesized via different technologies, such as sol-gel template method, chemical vapor deposition, and hydrothermal method. These methods are discussed in this paper, and the recent development of the synthesis technologies is also presented. Furthermore, the organic pollutants, degradation using the synthesized 1D TiO_2 nanostructures is studied as an important application of photocatalytic oxidation (PCO). The 1D nanostructured TiO_2 exhibited excellent photocatalytic activity in a PCO process, and the mechanism of photocatalytic degradation of organic pollutants is also discussed. Moreover, the modification of 1D TiO_2 nanostructures using metal ions, metal oxide, or inorganic element can further enhance the photocatalytic activity of the photocatalyst. This phenomenon can be explained by the suppression of e^--h^+ pairs recombination rate, increased specific surface area, and reduction of band gap. In addition, 1D nanostructured TiO_2 can be further constructed as a film or membrane, which may extend its practical applications.

1. Introduction

Organic pollutants are widely presented in wastewater, which have negative effects on environment and human health. Even developing water treatment technology calls for efficient decontamination method for complete degradation of persistent organic pollutants (POPs) [1–3]. Conventional biological, physical, and chemical processes have been employed and have showed capability in degrading most organic pollutants, while for POPs, complete degradation is still a big challenge. Advanced oxidation process (AOP) has thus developed by oxidization with hydroxyl radicals (•OH), which are provided by introducing ozone, hydrogen peroxide, and UV irradiation. However, complete degradation of POPs is still difficult due to the ease in forming disinfection by-products.

TiO_2-mediated semiconductor photocatalysis has attracted considerable attention in view of their excellences in complete degradation of organic pollutants via photocatalytic oxidation (PCO) process. A general mechanism is illustrated in Figure 1 [4]. Initially, PCO process is triggered by the excitation of TiO_2 under the irradiation of photons with energy greater than the band-gap energy of TiO_2. The photogenerated electron (e^-) and holes (h^+) pairs without recombination can migrate to TiO_2 surface to participate in redox reactions with adsorbed species with the possible formation of superoxide radical anion ($\bullet O_2^-$) and hydroxyl radical (•OH), respectively. These reactive oxygen species are mainly responsible for the degradation of organic pollutants in water. Furthermore, the excitation of TiO_2 by UV light can be displayed in the following equations [5–8]:

$$TiO_2 + h\nu\,(\lambda < 387\,\text{nm}) \longrightarrow e^- + h^+ \quad (1)$$

$$e^- + O_2 \longrightarrow O_2^{\bullet -} \quad (2)$$

In an organic degradation process, the formed e^- and h^+ act as reductant and oxidant, respectively. The reaction steps are represented as follows [6].

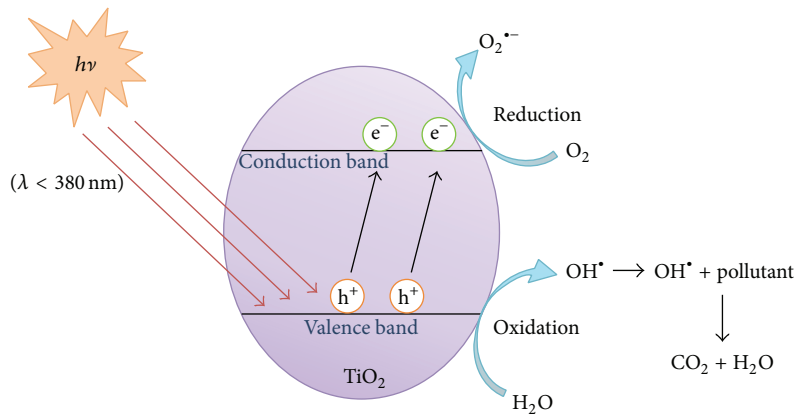

Figure 1: General mechanism of the photocatalysis [13].

Table 1: Typical synthetic methods of 1D TiO_2 nanostructures.

TiO_2 nanostructures	Synthesis methods	References
TiO_2 nanorods	Sol-gel template method	[20]
	Hydrothermal method	[22]
	Chemical vapor deposition	[23]
TiO_2 nanotubes	Electrochemical deposition	[37]
	Template method	[41, 42]
	Hydrothermal method	[39, 44–46]
TiO_2 nanowires/nanofibers	Hydrothermal method	[5]
	Microwave	[75]
	Electrospinning	[76]
TiO_2 nanobelts	Solvothermal method	[65]
	Chemical vapor deposition	[68]
	Hydrothermal method	[67]

Oxidative Reaction:

$$h^+ + \text{Organic (R)} \longrightarrow \text{Intermediates} \longrightarrow CO_2 + H_2O \quad (3)$$

$$h^+ + H_2O \longrightarrow \bullet OH + H^+ \quad (4)$$

Reductive Reaction:

$$\bullet OH + \text{Organic (R)} \longrightarrow \text{Intermediates} \longrightarrow CO_2 + H_2O \quad (5)$$

Current research progress has shown that TiO_2-based materials demonstrate highly active photocatalytic degradation of different organic pollutants [9–11]. For example, phenol, chlorinated aromatics, and aniline compounds are susceptible to oxidation by TiO_2, and they can form intermediate radicals that may subsequently trigger a series of radical reactions in this process. Due to the excellent oxidation ability, the resulting intermediates can be finally degraded into CO_2 and H_2O. Since the oxidation process is primarily driven by electron transfer reactions at the surface of TiO_2, the specific surface area of TiO_2 is an important factor which can affect the PCO efficiency.

To significantly boost the photoenergy conversion efficiency, tailing nanostructured TiO_2 has attracted continuous research interest, among which one-dimensional (1D) nanostructures possessing large surface areas and unique physical and chemical specificities are of particular interest [12]. Various 1D nanostructures including nanorods, nanowires/nanofibers, nanotubes, and nanobelts have been successively synthesized during the past decades. Some typical synthetic methods of 1D TiO_2 nanostructures are summarized in Table 1. Nanorods have a low aspect ratio (length divided by width) ranging from 3 to 5. Nanotubes are a type of nanometer-scale tube-like structure, which have a similar size with nanorods. For the nanowires/nanofibers, they have a higher aspect ratio as compared to nanorods. Nanobelt is a nanostructure in a form of belt. The specific geometry with high aspect ratio renders dramatical enhancements in charge carrier generation, transport, and separation, boosting the photoenergy conversion efficiency [13, 14]. Up to now 1D TiO_2 has been comprehensively investigated for the degradation of organic pollutants, such as dyes, POPs (phenol and derivatives) and natural organic matters (NOMs) [15, 16].

2. TiO_2 Nanorods

TiO_2 nanorods have a relatively small amount of grain boundaries and can act as single crystal, which is able to reduce the grain boundary effect and provide fast

electron transport [17]. Previous reports indicated that TiO_2 nanorods exhibited higher photocatalytic activity than nanoparticle counterparts due to the increased numbers of active sites and crystal plane effects [18]. Furthermore, TiO_2 nanorods have lower recombination rate of e^- and h^+ as compared with TiO_2 nanoparticles, which would enhance the photocatalytic activity of the photocatalyst [19].

Various synthetic strategies have been designed for the preparation of TiO_2 nanorods, which include sol-gel template method, chemical vapor deposition (CVD), and hydrothermal method [19–23].

Attar et al. [20] developed an improved sol-gel template method for the synthesis of TiO_2 nanorods, as shown in Figure 2(a). Anodic alumina membranes (Figure 2(a)) were applied as the template with pore sizes ranging from 50 to 300 nm. Owing to the adjustable membrane pore sizes, the diameter of the synthesized TiO_2 nanorods can be controlled. Figure 2(b) shows the synthesized TiO_2 nanorods with diameter of 160–250 nm, revealing that the nanorods synthesized via this method have a uniform diameter as well as a smooth surface. However, they found that the diameter of the synthesized TiO_2 nanorods was much smaller than the pore size of the template, which was attributed to the densification and lateral shrinkage of the template during the annealing process.

Wu and Yu synthesized a novel type of well-aligned rutile and anatase TiO_2 nanorods via a template-free metal-organic CVD method [21]. As shown in Figure 2(c), TiO_2 nanorods were grown directly on a silicon substrate at a temperature of 500–700°C. The single-crystalline rutile and anatase TiO_2 nanorods were formed at 630°C and 560°C, respectively, which indicated that the temperature was a key factor in the synthesis process. The disadvantage of this method is the complicated synthesis process, which is not suitable for production in large-scale.

Hydrothermal method is facile for the synthesis of 1D nanostructured TiO_2 [22]. Feng et al. [22] developed a new type of nanorod film on glass substrates via a low-temperature hydrothermal process. As shown in Figure 2(d), the nanorods have diameters of 30–60 nm and they have uniform orientation. Furthermore, the authors found that the surface of the synthesized film has switchable wettability which transferred from superhydrophobicity to superhydrophilicity under UV light irradiation. This phenomenon can be explained by the reaction between the photogenerated holes and the lattice oxygen, leading to the formation of surface oxygen vacancies.

TiO_2 nanorods have been widely used in PCO process for the degradation of organics [24]. For example, organic dyes and acetone can be effectively degraded into CO_2 and H_2O. Melghit and Al-Rabaniah [24] prepared rutile TiO_2 nanorods using a sol-gel method at room temperature, and the material exhibits excellent photodegradation of Congo red under sunlight. It can be explained by two aspects. (1) The Congo red is easily absorbed onto the synthesized TiO_2 nanorods, and, subsequently, the dye decomposed in a PCO process. (2) Organic dyes are capable of photosensitizing TiO_2 because of the absorption of visible light [25]. The photosensitization was considered as another way for the degradation of dyes in the presence of TiO_2 under sunlight irradiation. It was worth noting that the synthesized rutile TiO_2 nanorods which possess optimum size and shape are much more efficient for PCO process than the anatase TiO_2 [24]. Yu and coworkers [26] synthesized TiO_2 nanostructures using TiF_4 and H_3BO_3 as the precursors. The morphology characterization revealed that the synthesized material is a combination of TiO_2 nanorods and nanotubes. It is important to notice that the synthesized TiO_2 exhibited a higher PCO efficiency for the degradation of acetone than that of P25 due to the larger specific surface area and pore volume of the synthesized TiO_2. Moreover, compared with the nanosized powder photocatalysts, the prepared TiO_2 is easier to be separated from aqueous solutions after PCO process due to its long structure, and it also possesses higher photocatalytic activity. In addition, the photocatalytic activity of TiO_2 nanorods can be further improved via a thermal treatment because of the enhanced crystallization [27].

In order for facile recycling, TiO_2 nanorods have been coated onto substrates. A successful example is that well-aligned TiO_2 nanorod can be prepared on pretreated quartz substrate [28]. The quartz substrate was precoated with a thin rutile TiO_2 seed layer to facilitate the subsequent growth of the rutile TiO_2 nanorods. Owing to the excellent nucleation and growth properties, rutile TiO_2 crystal seeds are more preferable than anatase TiO_2. Thus, the pretreatment of substrates is important for the synthesized TiO_2 morphology, which would also affect the performance of the material in a PCO process. Based on the experimental results, the density of TiO_2 seeds can be controlled by the concentration of the coating colloid solution. Then the TiO_2 crystal seeds will affect the growth density, diameter distribution, and growth morphologies of TiO_2 nanorods. When the density of TiO_2 seeds is high, the seeds tend to merge together to form larger TiO_2 particles. It is shown that the degradation rates of methyl blue increased with large growth density and small diameter size of TiO_2 nanorods.

Pure TiO_2 is not an effective visible-light photocatalyst due to its wide band gap (>3.0 eV) and can be activated only by UV light at $\lambda \leq 380$ nm. Modification of TiO_2 has been explored to extend the absorption spectra of photocatalysts to visible light range [29]. Doping of TiO_2 with various metals or nonmetals has been considered as a valid way to lower the band gap of TiO_2 and thus make the photocatalyst more active under solar light. Doping of TiO_2 would introduce allowed energy states within the band gap but very close to the energy band. The gap between the energy states and the nearest energy band is usually reduced. Thus, the electrons and holes would be more easily excited under visible light irradiation. Kerkez and Boz [30] used Cu^{2+} as a dopant to modify TiO_2 nanorod array films (Figure 3(a)), and they found that the methylene blue degradation efficiency under visible light was increased 40% with respect to the efficiency of the unmodified sample. The notable improvement could be explained by the following factors. (1) Cu^{2+} acts as a trap

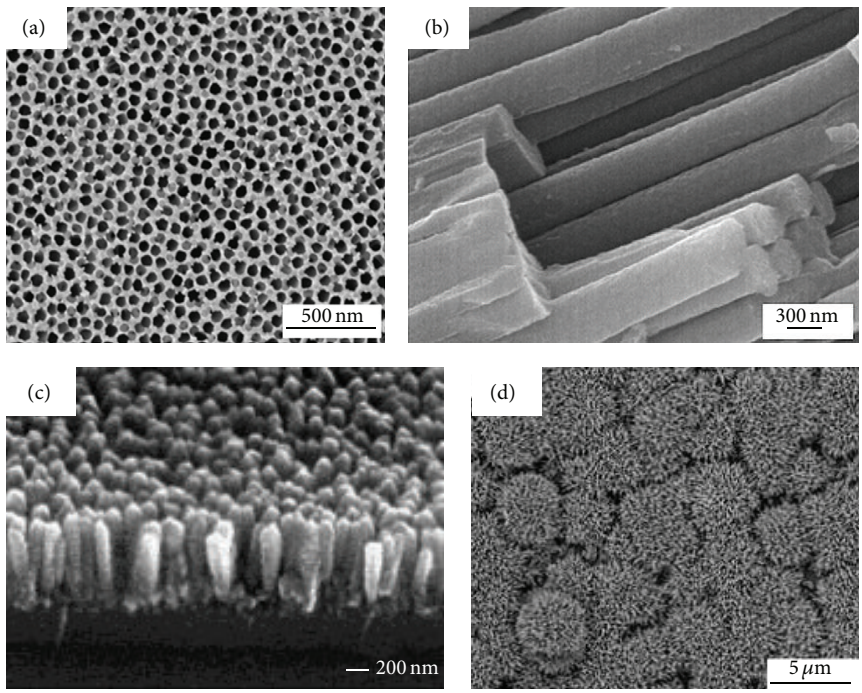

Figure 2: (a) FESEM image of the template (anodic alumina membrane) [20], (b) FESEM image of the synthesized TiO_2 nanorod arrays [20], (c) FESEM image of anatase TiO_2 nanorods [21], and (d) FESEM image of TiO_2 nanorod film [22].

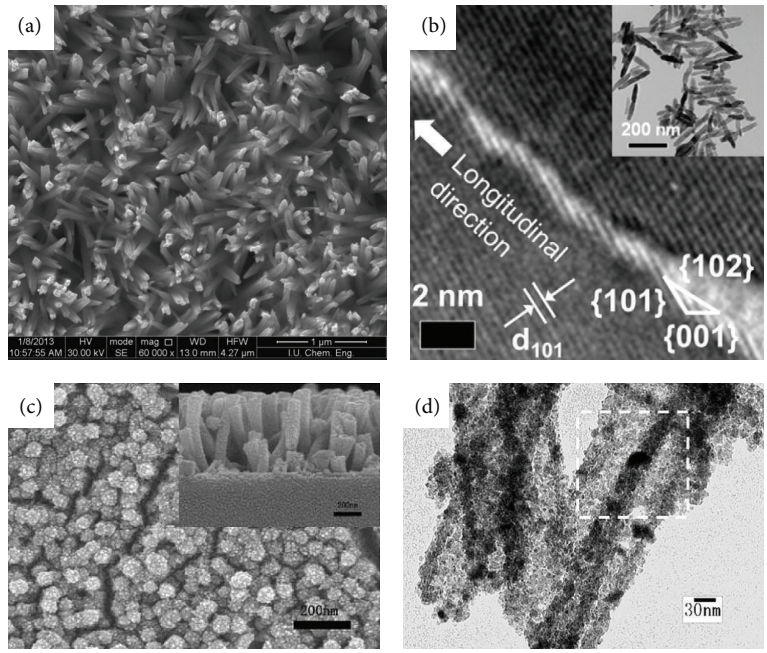

Figure 3: (a) SEM image of Cu^{2+}-TiO_2 nanorods, (b) TEM image of N-TiO_2 nanorods [31], (c) FESEM image of N-F-TiO_2 nanorods (inset: its cross section) [32], and (d) TEM image of Au-loaded TiO_2 hollow nanorods [33].

of photogenerated electrons. The electrons were transferred from TiO_2 to the conduction band of the CuO with little chance to return and thus increase the life time of e^--h^+. Thus, the presence of Cu^{2+} could retard the recombination rate of electrons and holes on the surface of the synthesized Cu^{2+}-TiO_2. (2) The band gap of Cu^{2+}-TiO_2 nanorods is lower than that of the original TiO_2, which can extend the photoresponse of the photocatalyst and make the material utilizable under both UV light and visible light.

TiO_2 nanorods with 3% of nitrogen doping were prepared by Lee and coworkers, as shown in Figure 3(b) [31]. Although the N-doping process did no change the morphology of TiO_2

nanorods, it provides extra occupied states above its valence band which may enhance the photocatalytic activity. Lv et al. also reported the synthesis of N-F-doped visible light active TiO_2 nanorods via a liquid phase deposition process (Figure 3(c)) [32]. They firstly synthesized ZnO nanorod arrays on glass substrates and then combined the ZnO nanorod arrays and TiO_2 via an aqueous solution method to get the as-prepared TiO_2 nanorods. Their experimental results indicated that the doping quantity of N and F in the resultant material could be easily controlled by adjusting the calcination temperature, and the optimal temperature was found to be 450°C. Owing to the higher visible light photocatalytic activity, the obtained TiO_2 nanorods' films exhibited higher degradation rate for methylene blue as compared to P25 films [32].

Metals have been incorporated into TiO_2 nanorods to form nanocomposites with a heterojunction structure. For example, TiO_2 nanorods can be coated by Au nanoparticles to form a novel heterojunction, as shown in Figure 3(d) [33]. As a model organic pollutant, methylene blue can be used to characterize the photocatalytic activity of the synthesized photocatalysts. 35% of methylene blue was degraded in the presence of Au-TiO_2 nanorods, which is much more effective than that of 15% for pure nanorods. In addition, the other metals such as Ag and Cu can also be coated onto TiO_2 nanorods [34, 35]. The synthesized nanocomposites exhibited outstanding photocatalytic activity as compared to the pure TiO_2. The enhancement in photocatalytic activity is related with the slow recombination rate of charge carriers. During PCO process, the generated electrons from TiO_2 nanorods could transfer to Au nanoparticles, leading to the longer lifetime of the e^--h^+ pairs and therefore more reactive oxygen species produced for the degradation of organic pollutants in water. The mechanism of photocatalytic degradation of organic pollutants over metal/TiO_2 under UV light irradiation is shown in Figure 4.

3. TiO_2 Nanotubes

Currently, TiO_2 nanotube structures have been successfully synthesized and applied for organic pollutants degradation [36]. Hoyer [37] firstly reported the synthesis of TiO_2 nanotubes via an electrochemical deposition in a porous aluminum oxide mold. Then, an electrochemical anodic oxidation method was developed by Zwilling et al. for the synthesis of TiO_2 nanotubes [38]. Although this method is very facile to synthesize TiO_2 nanotubes with controllable pore size, good uniformity, and conformability over large areas, the high cost of fabrication apparatus and complicated operation limited its further application [39, 40]. Templating method was considered as a suitable technology to construct materials with desirable morphology [41]. TiO_2 nanotubes can be synthesized in controlled sol-gel hydrolysis of solutions containing titanium compounds and templating agents followed by polymerization or deposition of TiO_2 on the template. For example, Peng and coworkers [42] fabricated TiO_2 nanotubes via a surfactant-mediated templating method, and the fabrication process can be summarized in Figure 5. In the synthesis process, a sol-gel method was conducted for fabricating the material, and laurylamine hydrochloride (LAHC) was used as a template. Titanium alkoxide was first hydrolyzed with the addition of tetra-n-butyl-orthotitanate (TBOT), and then there is an interaction between partially charged hydrolytic species and laurylamine surfactant by H-bonding forces (Figure 5(a)). The edge part of the bilayer assemblies of LAHC was unstable and apt to combine with the interlayers, which lead to the enlargement of the layers (Figure 5(b)). Then the bilayer-like aggregates rearranged into lamellar-like liquid-crystal phases through the condensation reaction (Figure 5(c)). After the interlayer combination and crosslinking between adjacent hydrolyzed titanium alkoxide species, a mixed lamellar liquid-crystal phase membrane formed, and rodlike micelles were separated by bilayers of surfactant and water (Figure 5(d)). Upon the addition of TBOT, charge imbalance leads to the curvature of the membrane along one direction (Figure 5(e)) and then bends fully the membrane into tubules (Figure 5(f)). Moreover, the condensation of the hydrolyzed titanium species would lead to the rodlike micelles in a random arrangement (Figure 5(g)). The synthesized TiO_2 nanotubes possess a hierarchical tubules-within-tubules structure with cylindrical nanochannels walls. This structure is a combination structure of microtube and nanotube, causing the formation of porous structure. Moreover, the specific surface area of the material is also increased. The structure would be beneficial for catalysts and thus enhance the PCO efficiency. Furthermore, the scale of the synthesized TiO_2 nanotubes can be controlled by adjusting the morphology of the template [41]. However, the instability of the TiO_2 nanotubes synthesized by this method is a big issue, and the tube morphology is easily destroyed [39, 40, 43].

Recently, hydrothermal method has been widely used for the synthesis of high quality of TiO_2 nanotubes with diameter of about 10 nm [44]. Crystalline TiO_2 nanoparticles and highly concentrated NaOH are normally used as the precursors in a typical hydrothermal process [41]. As a necessary step, the drying or calcination process is generally conducted, leading to the transformation of titanate nanotubes to TiO_2 nanotubes. Based on previous reports [39, 45, 46], the advantages of hydrothermal process for TiO_2 nanotubes synthesis can be concluded as the following. (1) It is suitable for large scale production; (2) the modification process of TiO_2 nanotubes can be directly conducted in the synthetic system; (3) nanotubes with ultrahigh aspect ratio can be synthesized. However, hydrothermal process requires high temperature and pressure, as well as the long reaction time, which also cause a high cost. Figure 6 lists various TiO_2 nanotubes synthesized by different methods.

TiO_2 nanotubes can be used for the degradation of POPs such as benzene and acetaldehyde [47, 48]. Yuan et al. [49] studied the performance of TiO_2 nanotubes for water treatment. The synthesized TiO_2 nanotubes showed complete photodegradation of humic acid in comparison to the 97.7% removal efficiency of TiO_2 P25. Moreover, the TiO_2 nanotubes can be totally separated and recovered via a membrane filtration. The stability test presented that no catalyst deactivation was observed after five consecutive

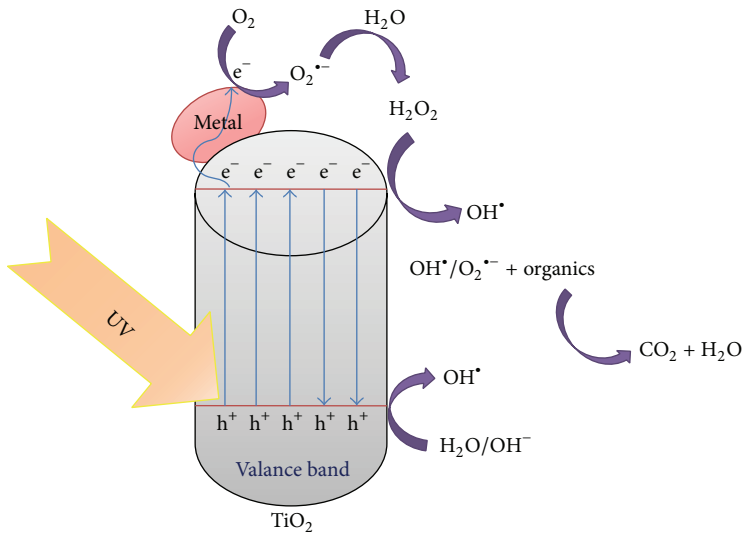

FIGURE 4: The mechanism of photodegradation of organic pollutants over metal/TiO_2 in water under UV light irradiation.

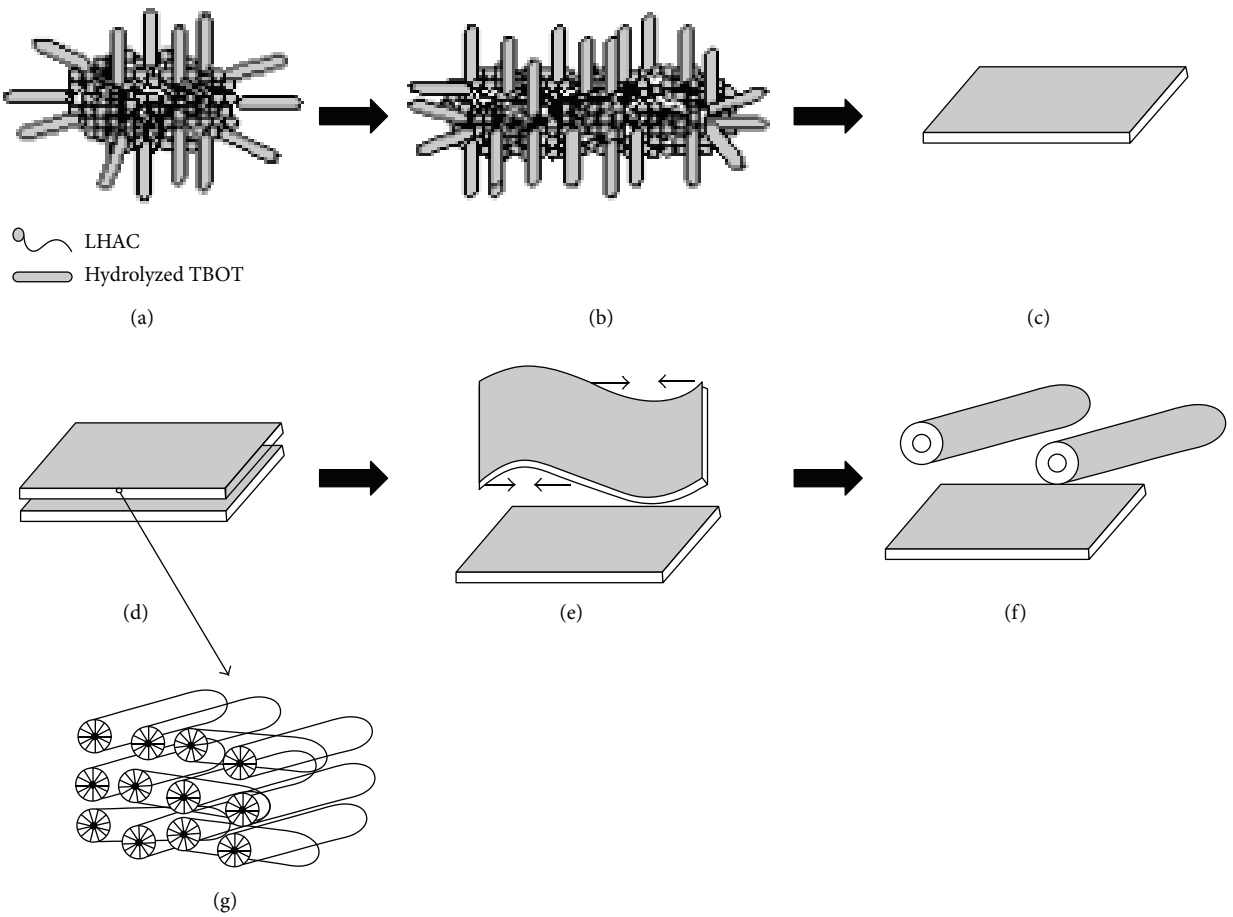

FIGURE 5: Proposed formation processes of the microtubules. (a) Globular aggregates containing LAHC and hydrolyzed TBOT. (b) Aggregates enlarged in size. (c) and (d) Mixed lamellar liquid-crystal phase membrane containing rodlike micelles. (e) Charge imbalance resulting in membrane curvature. (f) Further bending into tubules. (g) Random and segregated arrangement of rod micelle layers which are separated by bilayers of LAHC from bulk solution [42].

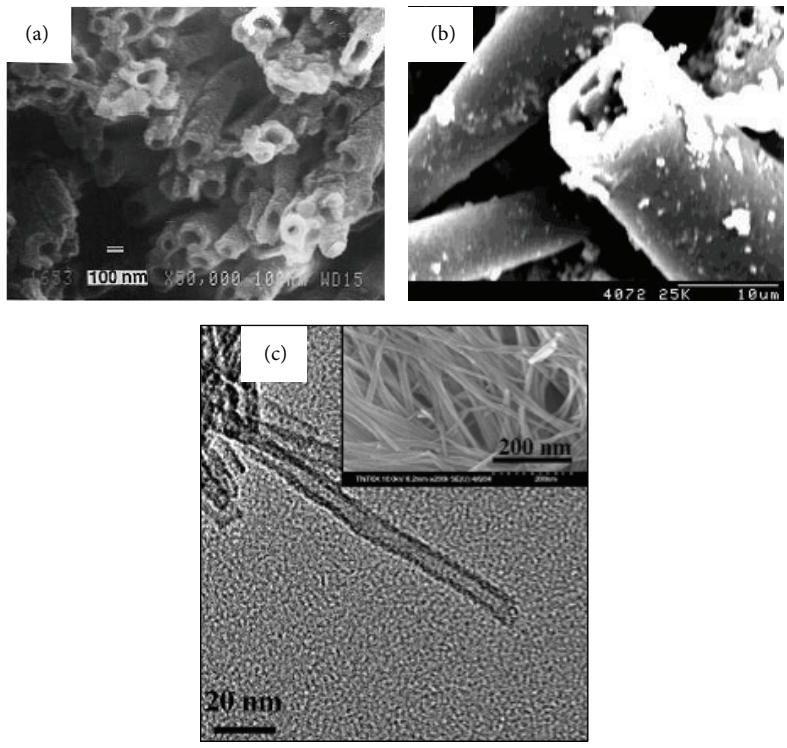

Figure 6: SEM image of TiO_2 nanotubes synthesized via an electrochemical deposition (a) [37] and templating methods (b) [42]; (c) FESEM (inset) and TEM images of TiO_2 nanotubes synthesized via a hydrothermal method [74].

PCO experiments of newly added humic acid. Yuan et al. [49] degraded humic acid using an enhanced photocatalytic process with Al and Fe codoped TiO_2 nanotubes as photocatalysts. They reported that calcination temperature, doping ions, and dosage of dopant would impact the PCO efficiency. Under an optimal condition of 1.0% codoped TiO_2 nanotubes containing 0.25 : 0.75 of Al : Fe, 79.4% of humic acid was degraded and a pseudo-first-order rate constant of $0.172\,min^{-1}$ was achieved. Bisphenol A (BPA) is a pervasive chemical intermediate primarily from the production of polycarbonate plastics and epoxy resin [50]. Over the past few years, considerable effort has been devoted to the development of effective treatment technologies of the removal for bisphenol A (BPA), such as Fenton's reagent, ultrasonic cavitation, photocatalysis, and ozonation [51]. Recent research [52] displayed that a nearly complete removal of BPA was observed by Cu doped TiO_2 nanotubes. The pseudo-first-order rate constants for BPA photodegradation by Cu doped TiO_2 nanotubes at pH 7.0 were 2–5 times higher than that of pure Degussa P25. In a typical process, the generated electrons from TiO_2 with a lower conduction band could recombine with the holes in Cu, resulting in the reduction of recombination rate of electrons and holes. Then, the holes and electrons reacted with water and oxygen to form peroxyl and hydroxyl radicals, respectively. In a supposed BPA degradation process, BPA radicals were generated via an electron transfer process. Subsequently, the BPA radicals triggered a suite of reactions of radical coupling, fragmentation, substitution, and elimination, which eventually resulted in degradation of BPA [53]. However, further study is needed to prove this mechanism. BPA molecules were firstly photodegraded into some intermediates and products with smaller molecular weight, and these intermediates can be further oxidized to CO_2 and H_2O by the oxidative species produced in the PCO process. N-doped TiO_2 nanotubes also showed enhanced photocatalytic activity. Based on the research work of Chen and coworkers [54], 72.5% and 89.4% of methyl orange are photodegraded in the presence of TiO_2 nanotubes and N-doped TiO_2 nanotubes, respectively. In addition, the degradation rate of methyl orange over TiO_2 nanotubes without calcination is only 17.1%, which is lower than that (45.1%) of TiO_2 nanotubes calcined at 200°C. This is due to the narrow band gap and good crystallinity [55]. However, the photocatalytic activity of the TiO_2 nanotubes calcined at 400°C decreased, which can be attributed to the agglomeration and sintering damage of nanotubes caused by calcination at high temperature [56]. The specific surface area of the calcined material may also decrease due to the destruction of the nanotube structure.

4. TiO_2 Nanowires/Nanofibers

TiO_2 nanowires/nanofibers are common nanostructures of TiO_2, as shown in Figure 7. Fujishima et al. [5] prepared two kinds of TiO_2 nanowires (TNW_{10} and TNW_{20}) for the degradation of humic acid. The investigation of photocatalytic activities of the synthesized materials showed that TNW_{10} performed better than TiO_2 P25 while TNW20

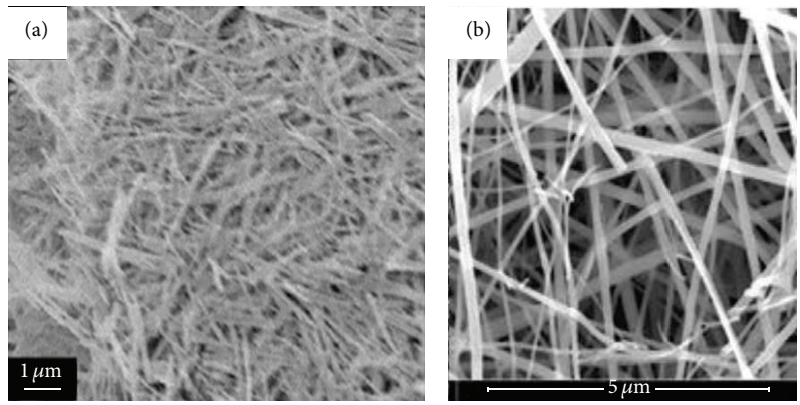

Figure 7: (a) FESEM of TiO_2 nanowires synthesized via a hydrothermal process [5], (b) FESEM of TiO_2 nanowires synthesized via an electrospun process [63].

was as good as P25. This is due to the high ratio aspect of the synthesized TiO_2 nanowires. Owing to the incomplete degradation, the degradation rates of total organic carbon content are lower than the removal rate of humic acid. This problem can be addressed by extending reaction time. Furthermore, the nanowires can be totally separated by a commercial microfiltration membrane with negligible membrane fouling. Pirilä and coworkers [57] studied the photocatalytic degradation of butanol in aqueous solutions using commercial TiO_2, N-Pt-doped TiO_2 nanofibers, and N-Pd-doped TiO_2 nanofibers. The experimental results showed that the N-Pd-doped TiO_2 nanofibers had high efficiency in the degradation of butanol under UV irradiation as compared to the N-Pt-doped TiO_2 nanofibers and the commercial TiO_2. It probably has relationship with the proton formation caused by better radical formation ability. GC-MS analysis revealed that butanol converted to some decomposition products such as aldehydes and ethanol [58]. Moreover, the synthesized materials had very similar BET surface area whereas they expressed relatively different reaction rate of the photocatalytic degradation, and it can be concluded that the specific surface area of the photocatalysts is not a key factor for the photocatalytic efficiency, while the doped metals played an important role in promoting the PCO reaction. In addition, Zn^{2+} doped TiO_2 nanofibers can be synthesized by electrospinning followed by calcination process [59]. The different dosage of Zn^{2+} would affect the photodegradation rate of methylene blue. For example, 96.1% of methylene blue was removed in the presence of TiO_2 nanofibers with 2 at.% Zn^{2+}, which was considered as an optimum doping dosage. Furthermore, the synthesized nanofibers were successfully recycled and reused for five times with little photocatalytic activity reduced. TiO_2 nanowires can also combine with other nanostructures, which can enhance the photocatalytic activity. Fe_2O_3 nanoparticles have been grafted onto TiO_2 nanowires by Qin and coworkers via a facile impregnation–solvothermal method [60]. The synthesized heterojunctions exhibited remarkable photocatalytic activity for photocatalytic oxidation of Direct Red 4BS in the presence of H_2O_2. Moreover, the material showed good tolerance with respect to organic matter poisoning due to the synergetic effect of TiO_2 nanowires and Fe_2O_3 nanoparticles. The size of Fe_2O_3 also affected the performance of the material, and it can be controlled by adjusting the impregnation duration time in the synthesis process. The possible reaction pathways are shown as follows [60]:

$$TiO_2 + h\nu \longrightarrow h + e^- \quad (6)$$

$$h^+ + H_2O \longrightarrow \bullet OH + H^+ \quad (7)$$

$$\equiv Fe^{III} + e^- \longrightarrow \equiv Fe^{II} \quad (8)$$

$$\equiv Fe^{II} + H_2O_2 \longrightarrow \equiv Fe^{III} + \bullet OH + OH^- \quad (9)$$

$$\bullet OH + 4BS \longrightarrow \bullet\bullet\bullet \longrightarrow CO_2 + H_2O \quad (10)$$

where the 4BS stands for the dye molecule and the $\bullet\bullet\bullet$ stands for the produced intermediates.

The heterojunction of TiO_2 nanofibers and Fe_2O_3 nanoparticles can promote the separation of photogenerated e^- and h^+. The conduction band of Fe_2O_3 is more active as compared to that of TiO_2, leading to the electrons transfer from TiO_2 to Fe^{III} and the further conversion to Fe^{II}. Since Fe^{II} promotes the decomposition of H_2O_2 to •OH [61], the photocatalytic activity was enhanced in this charge transfer process.

Liu and coworkers [62] prepared another kind of core-shell heterojunctions (TiO_2-B nanowires and anatase nanocrystals) using a combination of hydrothermal and calcination methods. Similarly, the charge recombination rate was suppressed. The synthesized material tends to separate the e^- and h^+ into two different regions of the catalyst and thus enhances photocatalytic efficiency [63].

Recently, TiO_2 nanowire membranes were fabricated and applied for organics degradation in water purification process due to their photocatalytic activity, excellent chemical resistance, and thermal stability [64–66].

Microfiltration and ultrafiltration membranes have been successfully synthesized by Zhang and coworkers. The membranes were fabricated by TiO_2 nanowires with different

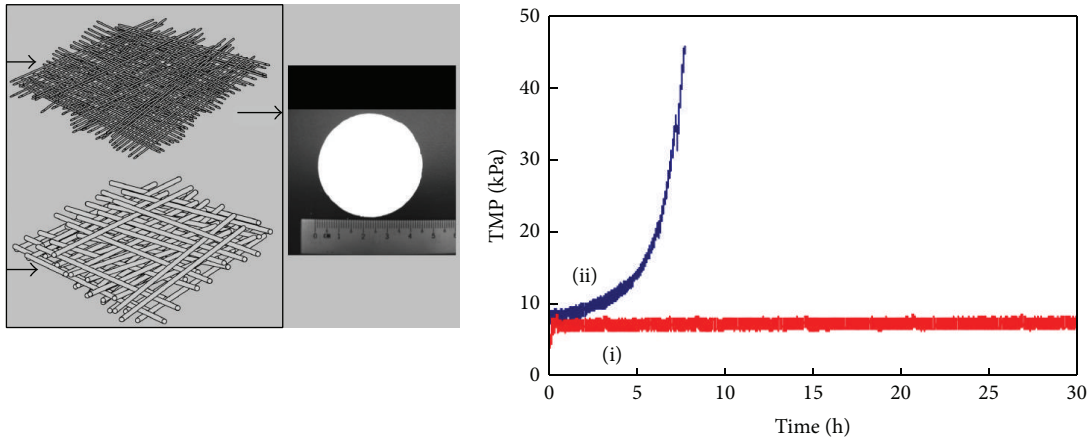

FIGURE 8: (a) TiO_2 nanowire membrane. (b) The transmembrane pressure change of TiO_2 nanowire membrane during filtration: (i) with UV irradiation and (ii) without UV irradiation.

diameters. In a typical synthesis process, The TiO_2 nanowires' suspension was first filtered via a vacuum filtration setup to form a porous functional layer. After drying at 105°C, a free-standing membrane can be peeled off from the filter. Finally, the membrane was pressurized under 5 bar at 120°C via a hot-press before being calcined at 550°C. As shown in Figure 8(a) [64], the synthesized membranes were robust and flexible and they possess multifunctions. In continuous experiments, the synthesized TiO_2 microfiltration nanowire membrane achieved near 100% and 93.6% removal rate of humic acid and total organics carbon, respectively. It is important to notice that the transmembrane pressure of the nanowire membrane did not change under UV light irradiation (Figure 8(b), [66]), indicating the antifouling and self-cleaning property of the synthesized TiO_2 nanowire membrane. The organic pollutants can be degraded concurrently during the filtration process. For a TiO_2 nanowire ultrafiltration membrane, the membrane showed a higher separation ability as well as excellent photocatalytic activity due to the enhanced selectivity. The rejection rate of humic acid by the ultrafiltration membrane can be achieved till 65% without UV irradiation, and even the bacteria (*E. coli*) can be intercepted by the membrane. In addition, the synthesized membranes were capable of overcoming the polymeric membrane problems such as membrane fouling and high-temperature applications. The antifouling property would facilitate the regeneration of the membrane and thus lower the cost for membrane cleaning.

TiO_2 nanowires membrane can also apply for the degradation of pharmaceuticals in water [65]. The membrane was directly fabricated by hydrothermal growth on Ti substrates at 180°C with the assistance of some organic solvents. Experimental details revealed that various pharmaceuticals such as norfluoxetine, atorvastatin, lincomycin, and fluoxetine were almost completely removed in a concurrent filtration and PCO process.

5. TiO_2 Nanobelts

TiO_2 nanobelts can be synthesized via CVD, solvothermal, and hydrothermal methods [67–69]. Gao and coworkers [69] reported the self-catalytic growth of codoped TiO_2 nanobelts via a metallorganic CVD method, and they found that rutile structure is dominant in the synthesized material. Furthermore, the material exhibited a magnetic anisotropy with a high coercive field value at room temperature. This property may facilitate the separation of the synthesized material after PCO process.

A solvothermal process was carried out to synthesize nitrogen-fluorine codoped TiO_2 (N-F-TiO_2) by He et al. [67]. Amorphous titania microspheres were used as precursors, which were prepared by the hydrolysis of $Ti(OBu)_4$. The synthesized N-F-TiO_2 nanobelts showed higher photocatalytic activity for the degradation of methyl orange as compared to that of TiO_2 P25. As shown in Figure 9, the codoped nanobelts photocatalyst exhibited the highest decrease in COD values for the degradation of organic compounds under both visible light and UV irradiation. This phenomenon can be attributed to the porous structures of the synthesized N-F-TiO_2, the increased specific surface area, and enhanced light adsorption. The N-F doping induced oxygen vacancy and led to the red shift in optical energy gap. Moreover, the nanobelt structure of the synthesized material would facilitate the capture of photogenerated photons and thus promote the formation of e^--h^+.

Hydrothermal methods are more commonly used for TiO_2 nanobelts synthesis [70–72]. A commercial P25 TiO_2 can be used as a precursor, which is subsequently hydrothermally treated for nanobelts synthesis, as shown in Figure 10(a) [70]. However, the photocatalytic activity of the synthesized TiO_2 nanobelts was lower than that of P25. The degradation rates of methyl orange are 35% and 95% in the presence of

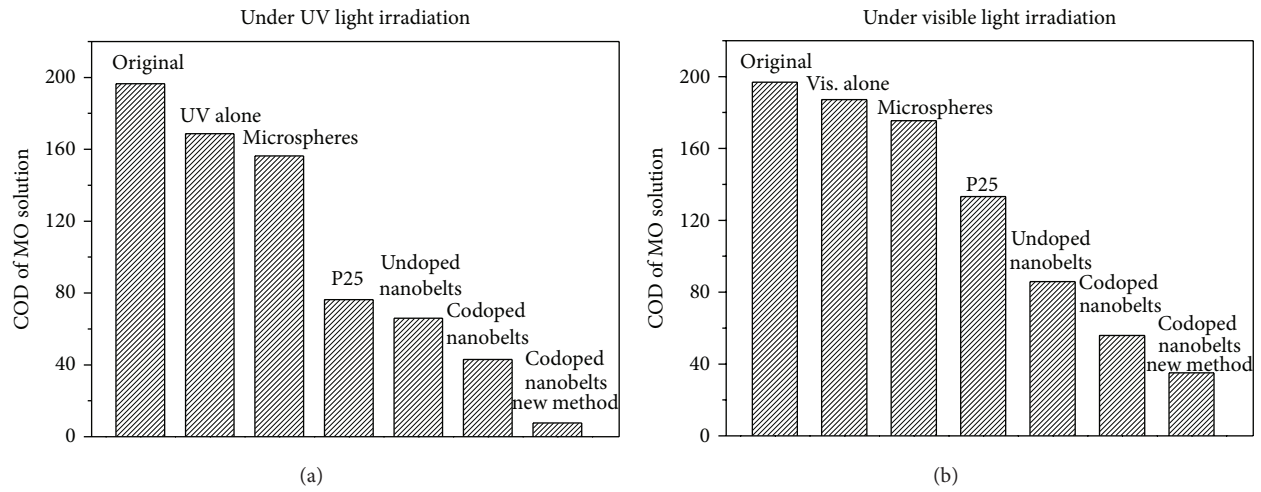

Figure 9: COD removal of the methyl orange solution after the photocatalytic degradation under UV and visible light irradiations [67].

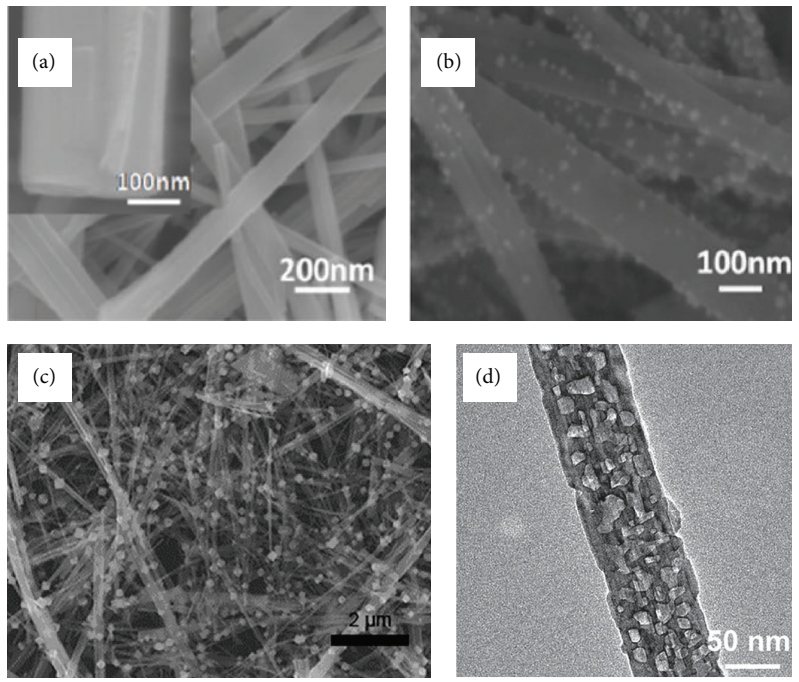

Figure 10: (a) SEM image of TiO_2 nanobelts synthesized via a hydrothermal process [70], (b) SEM image of NiO/TiO_2 heterojunctions [64], (c) SEM image of the Cu_2O/TiO_2 heterojunctions [71], and (d) TEM image of the synthesized CeO_2/TiO_2 nanobelt heterojunction [72].

TiO_2 nanobelts and P25, respectively. To further enhance the performance of the material for organics degradation, NiO nanoparticles were successfully deposited onto the nanobelts, as shown in Figure 10(b). The synthesized materials were applied for the decomposition of methyl orange under ultraviolet light irradiation. Experimental results indicated that heterojunction NiO-TiO_2 nanobelts showed better performance for the methyl orange removal as compared to both pure NiO nanoparticles and TiO_2 nanobelts. It can be attributed to the increased specific surface area and extended e^--h^+ lifetime.

Similar with this kind of heterojunction, other meal oxides nanoparticles and TiO_2 nanobelts can also be combined together for the improvement of photocatalytic activity. Zhang et al. prepared Cu_2O/TiO_2 heterojunctions using a combination process of hydrothermal method and chemical precipitation method [71]. The TiO_2 nanobelt acted as a substrate, and the dosage of Cu_2O can be controlled by adjusting the concentration of the precursor (copper sulfate). Figure 10(c) shows that Cu_2O nanoparticles were evenly grafted onto the TiO_2 nanobelts. Moreover, the synthesized heterojunction possessed higher adsorbability as compared

to pure TiO_2 nanobelt. Although the photocatalytic activity of the synthesized material showed a little decrease, the decoloration activity of the material for organics was enhanced. This phenomenon is attributed to the strong adsorption of methyl orange molecules on the surface of Cu_2O with exposure of $\{1\ 1\ 1\}$ facets.

Tian et al. synthesized novel CeO_2/TiO_2 nanobelt heterojunctions via a facile hydrothermal process, as shown in Figure 10(d) [72]. Compared with TiO_2, the synthesized CeO_2/TiO_2 exhibited enhanced photocatalytic performance for the degradation of methyl orange due to the proposed capture-photodegradation release mechanism. During PCO process, methyl orange molecules were captured by CeO_2 nanoparticles, then degraded by photogenerated radicals, and finally released to the solution. Since the PCO process is mainly conducted at the surface of photocatalysts, the adsorption capacity of CeO_2 nanoparticles was found to be important for the performance of PCO process. The synthesized CeO_2/TiO_2 nanobelt heterojunctions possessed good stability, high activity, and recyclable properties.

TiO_2 nanobelts have been applied to photocatalyze the oxidation of pharmaceutical contaminants in wastewater. Liang and coworkers [73] prepared anatase phase TiO_2 nanobelts with 30–100 nm in width and 10 μm in length via a high temperature hydrothermal method. Their results showed that persistent pharmaceuticals such as malachite green, naproxen, carbamazepine, and theophylline can be efficiently photodegraded in the presence of the synthesized TiO_2 nanobelts. The photogenerated active oxygen species such as hydroxyl radical, h^+, and hydrogen peroxide were determined and it was proven that they played an important role in the PCO process. Investigation on operation parameters presented that photodegradation of the pharmaceuticals was evidently dependent on pH, illumination time, temperature, and concentrations of contaminants. This work heralds a pathway towards the photodegradation of organics in actual wastewater. TiO_2 nanobelts can have potential in applications of industrial wastewater.

6. Conclusions

This review paper overviews the recent development in synthesis of 1D TiO_2 nanostructures and their photocatalytic applications for organics degradation. Thanks to the development of nanotechnology, significant progress has been achieved in controllable synthesis of 1D TiO_2 materials with different aspect ratio and inner structure (solid nanowire, nanorod, nanobelt, and hollow nanotube). Various synthetic strategies have been developed, prompting the subsequent exploration of their photocatalytic properties and the practical environmental applications. Under the excitation of UV light, efficient degradation of organic pollutants, such as NOMs, POPs, dyes, phenols, and pharmaceuticals, has been achieved by numerous groups. On contrast, solar-light-active 1D TiO_2 material is still in its infant stage. Since solar energy is economical, solar photocatalysis using 1D TiO_2 nanostructures would be a promising pathway for the degradation of organic pollutants. It is important to note that the application of 1D TiO_2 in industry cannot be successful without solar energy assistance. Thus, many future works should concentrate on the synthesis of solar-light-active TiO_2 materials. Doping of 1D TiO_2 is considered as a possible way to lower the band gap of TiO_2 and thus enhance the activity of TiO_2 under solar light. Moreover, sensitization of 1D TiO_2 nanostructures with other narrow-band-gap semiconductor and noble metals (e.g., Au or Ag) may further enhance the photocatalytic activity by suppressing the charge recombination rate.

Alternatively, 1D nanostructured TiO_2 materials can be used as building blocks to assemble active and integrated nanosystems, such as TiO_2 nanorod, nanotube, or nanowire membrane or film. The coupling of semiconductor photocatalysis of 1D nanomaterials and engineering design such as self-cleaning membrane filtration and microreactor construction might significantly broaden the application range of 1D TiO_2 photocatalysts. Rapid progress is expected and will mainly occur in developing economic and scalable synthetic strategy of 1D TiO_2 nanostructures and their industry-scale applications in water treatment process.

Conflict of Interests

The authors declare that there is no conflict of interests regarding the publication of this paper.

References

[1] G. T. Daigger, B. E. Rittmann, S. Adham, and G. Andreottola, "Are membrane bioreactors ready for widespread application?" *Environmental Science and Technology*, vol. 39, no. 19, pp. 399A–406A, 2005.

[2] M. A. Shannon, P. W. Bohn, M. Elimelech, J. G. Georgiadis, B. J. Marīas, and A. M. Mayes, "Science and technology for water purification in the coming decades," *Nature*, vol. 452, no. 7185, pp. 301–310, 2008.

[3] T. Zhang, X. Zhang, J. Ng, H. Yang, J. Liu, and D. D. Sun, "Fabrication of magnetic cryptomelane-type manganese oxide nanowires for water treatment," *Chemical Communications*, vol. 47, no. 6, pp. 1890–1892, 2011.

[4] M. Y. Ghaly, T. S. Jamil, I. E. El-Seesy, E. R. Souaya, and R. A. Nasr, "Treatment of highly polluted paper mill wastewater by solar photocatalytic oxidation with synthesized nano TiO_2," *Chemical Engineering Journal*, vol. 168, no. 1, pp. 446–454, 2011.

[5] A. Fujishima, T. N. Rao, and D. A. Tryk, "Titanium dioxide photocatalysis," *Journal of Photochemistry and Photobiology C*, vol. 1, no. 1, pp. 1–21, 2000.

[6] S. Ahmed, M. G. Rasul, R. Brown, and M. A. Hashib, "Influence of parameters on the heterogeneous photocatalytic degradation of pesticides and phenolic contaminants in wastewater: a short review," *Journal of Environmental Management*, vol. 92, no. 3, pp. 311–330, 2010.

[7] A. L. Linsebigler, G. Lu, and J. T. Yates Jr., "Photocatalysis on TiO_2 surfaces: principles, mechanisms, and selected results," *Chemical Reviews*, vol. 95, no. 3, pp. 735–758, 1995.

[8] T. Zhang, X. Yan, and D. D. Sun, "Hierarchically multifunctional K-OMS-2/TiO2/Fe3O4 heterojunctions for the photocatalytic oxidation of humic acid under solar light irradiation," *Journal of Hazardous Materials*, vol. 243, pp. 302–310, 2012.

[9] C. L. Bianchi, S. Gatto, C. Pirola et al., "Photocatalytic degradation of acetone, acetaldehyde and toluene in gas-phase: comparison between nano and micro-sized TiO_2," *Applied Catalysis B: Environmental*, vol. 146, pp. 123–130, 2013.

[10] J. Herrmann, "Heterogeneous photocatalysis: fundamentals and applications to the removal of various types of aqueous pollutants," *Catalysis Today*, vol. 53, no. 1, pp. 115–129, 1999.

[11] M. Stylidi, D. I. Kondarides, and X. E. Verykios, "Visible light-induced photocatalytic degradation of Acid Orange 7 in aqueous TiO_2 suspensions," *Applied Catalysis B: Environmental*, vol. 47, no. 3, pp. 189–201, 2004.

[12] M. M. Khin, A. S. Nair, V. J. Babu, R. Murugan, and S. Ramakrishna, "A review on nanomaterials for environmental remediation," *Energy and Environmental Science*, vol. 5, no. 8, pp. 8075–8109, 2012.

[13] X. Quan, S. Yang, X. Ruan, and H. Zhao, "Preparation of titania nanotubes and their environmental applications as electrode," *Environmental Science & Technology*, vol. 39, no. 10, pp. 3770–3775, 2005.

[14] X. Chen and S. S. Mao, "Titanium dioxide nanomaterials: synthesis, properties, modifications and applications," *Chemical Reviews*, vol. 107, no. 7, pp. 2891–2959, 2007.

[15] C. W. Lai, J. C. Juan, W. B. Ko, and S. B. A. Hamid, "An overview: recent development of titanium oxide nanotubes as photocatalyst for dye degradation," *International Journal of Photoenergy*, vol. 2014, Article ID 524135, 14 pages, 2014.

[16] F. Niu, L. Zhang, C. Chen et al., "Hydrophilic TiO_2 porous spheres anchored on hydrophobic polypropylene membrane for wettability induced high photodegrading activities," *Nanoscale*, vol. 2, no. 8, pp. 1480–1484, 2010.

[17] J. Qu and C. Lai, "One-dimensional TiO_2 nanostructures as photoanodes for dye-sensitized solar cells," *Journal of Nanomaterials*, vol. 2003, Article ID 762730, 11 pages, 2013.

[18] S. Liang, F. Teng, G. Bulgan, R. Zong, and Y. Zhu, "Effect of phase structure of MnO_2 nanorod catalyst on the activity for CO oxidation," *Journal of Physical Chemistry C*, vol. 112, no. 14, pp. 5307–5315, 2008.

[19] Y. Lia, M. Guo, M. Zhang, and X. Wang, "Hydrothermal synthesis and characterization of TiO_2 nanorod arrays on glass substrates," *Materials Research Bulletin*, vol. 4, pp. 1232–1237, 2009.

[20] A. S. Attar, M. S. Ghamsari, F. Hajiesmaeilbaigi, S. Mirdamadi, K. Katagiri, and K. Koumoto, "Sol-gel template synthesis and characterization of aligned anatase-TiO_2 nanorod arrays with different diameter," *Materials Chemistry and Physics*, vol. 113, no. 2-3, pp. 856–860, 2009.

[21] J. J. Wu and C. C. Yu, "Aligned TiO_2 nanorods and nanowalls," *Journal of Physical Chemistry B*, vol. 108, no. 11, pp. 3377–3379, 2004.

[22] X. J. Feng, J. Zhai, and L. Jiang, "The fabrication and switchable superhydrophobicity of TiO_2 nanorod films," *Angewandte Chemie International Edition*, vol. 44, no. 32, pp. 5115–5118, 2005.

[23] S. Feng, J. Yang, M. Liu et al., "CdS quantum dots sensitized TiO_2 nanorod-array-film photoelectrode on FTO substrate by electrochemical atomic layer epitaxy method," *Electrochimica Acta*, vol. 8, pp. 321–326, 2012.

[24] K. Melghit and S. S. Al-Rabaniah, "Photodegradation of Congo red under sunlight catalysed by nanorod rutile TiO_2," *Journal of Photochemistry and Photobiology A: Chemistry*, vol. 184, no. 3, pp. 331–334, 2006.

[25] F. Han, V. S. R. Kambala, M. Srinivasan, D. Rajarathnam, and R. Naidu, "Tailored titanium dioxide photocatalysts for the degradation of organic dyes in wastewater treatment: a review," *Applied Catalysis A: General*, vol. 359, no. 1-2, pp. 25–40, 2009.

[26] H. Yu, J. Yu, B. Cheng, and J. Lin, "Synthesis, characterization and photocatalytic activity of mesoporous titania nanorod/titanate nanotube composites," *Journal of Hazardous Materials*, vol. 147, no. 1-2, pp. 581–587, 2007.

[27] Q. Mu, Y. Li, Q. Zhang, and H. Wang, "Template-free formation of vertically oriented TiO_2 nanorods with uniform distribution for organics-sensing application," *Journal of Hazardous Materials*, vol. 188, no. 1–3, pp. 363–368, 2011.

[28] M. Gao, Y. Li, M. Guo, M. Zhang, and X. Wang, "Effect of substrate pretreatment on controllable growth of TiO_2 nanorod arrays," *Journal of Materials Science and Technology*, vol. 28, pp. 577–586, 2012.

[29] Q. L. Yu and H. J. H. Brouwers, "Design of a novel photocatalytic gypsum plaster: with the indoor air purification property," *Advanced Materials Research*, vol. 65, pp. 751–756, 2013.

[30] Ö. Kerkez and İ. Boz, "Photo(electro)catalytic activity of Cu^{2+}-modified TiO_2 nanorod array thin films under visible light irradiation," *Journal of Physics and Chemistry of Solids*, vol. 75, pp. 611–618, 2014.

[31] M. Lee, H. J. Yun, S. Yu, and J. Yi, "Enhancement in photocatalytic oxygen evolution via water oxidation under visible light on nitrogen-doped TiO_2 nanorods with dominant reactive 102 facets," *Catalysis Communications*, vol. 43, pp. 11–15, 2014.

[32] Y. Lv, Z. Fu, B. Yang et al., "Preparation N-F-codoped TiO_2 nanorod array by liquid phase deposition as visible light photocatalyst," *Materials Research Bulletin*, vol. 46, no. 3, pp. 361–365, 2011.

[33] H. Zhu, B. Yang, J. Xu et al., "Construction of Z-scheme type CdS-Au-TiO_2 hollow nanorod arrays with enhanced photocatalytic activity," *Applied Catalysis B: Environmental*, vol. 90, no. 3-4, pp. 463–469, 2009.

[34] M. Wu, B. Yang, Y. Lv et al., "Efficient one-pot synthesis of Ag nanoparticles loaded on N-doped multiphase TiO_2 hollow nanorod arrays with enhanced photocatalytic activity," *Applied Surface Science*, vol. 256, no. 23, pp. 7125–7130, 2010.

[35] J. Z. Y. Tan, Y. Fernández, D. Liu, M. M. Valer, J. Bian, and X. Zhang, "Photoreduction of CO_2 using copper-decorated TiO_2 nanorod films with localized surface plasmon behavior," *Chemical Physics Letters*, vol. 531, pp. 149–154, 2012.

[36] Y. Liu, B. Zhou, J. Bai et al., "Efficient photochemical water splitting and organic pollutant degradation by highly ordered TiO_2 nanopore arrays," *Applied Catalysis B: Environmental*, vol. 89, pp. 142–148, 2009.

[37] P. Hoyer, "Formation of a titanium dioxide nanotube array," *Langmuir*, vol. 12, no. 6, pp. 1411–1413, 1996.

[38] V. Zwilling, E. Darque-Ceretti, A. Boutry-Forveille, D. David, M. Y. Perrin, and M. Aucouturier, "Structure and physicochemistry of anodic oxide films on titanium and TA6V alloy," *Surface and Interface Analysis*, vol. 27, no. 7, pp. 629–637, 1999.

[39] N. Liu, X. Chen, J. Zhang, and J. W. Schwank, "A review on TiO_2-based nanotubes synthesized via hydrothermal method: formation mechanism, structure modification, and photocatalytic applications," *Catalysis Today*, vol. 225, pp. 34–51, 2014.

[40] D. Gong, C. A. Grimes, O. K. Varghese et al., "Titanium oxide nanotube arrays prepared by anodic oxidation," *Journal of Materials Research*, vol. 16, no. 12, pp. 3331–3334, 2001.

[41] D. V. Bavykin, J. M. Friedrich, and F. C. Walsh, "Protonated titanates and TiO_2 nanostructured materials: synthesis, properties, and applications," *Advanced Materials*, vol. 18, no. 21, pp. 2807–2824, 2006.

[42] T. Peng, A. Hasegawa, J. Qiu, and K. Hirao, "Fabrication of titania tubules with high surface area and well-developed mesostructural walls by surfactant-mediated templating method," *Chemistry of Materials*, vol. 15, no. 10, pp. 2011–2016, 2003.

[43] J. H. Jung, H. Kobayashi, K. J. C. van Bommel, S. Shinkai, and T. Shimizu, "Creation of novel helical ribbon and double-layered nanotube TiO_2 structures using an organogel template," *Chemistry of Materials*, vol. 14, no. 4, pp. 1445–1447, 2002.

[44] C. L. Wong, Y. N. Tan, and A. R. Mohamed, "A review on the formation of titania nanotube photocatalysts by hydrothermal treatment," *Journal of Environmental Management*, vol. 92, no. 7, pp. 1669–1680, 2011.

[45] T. Kasuga, M. Hiramatsu, A. Hoson, T. Sekino, and K. Niihara, "Formation of titanium oxide nanotube," *Langmuir*, vol. 14, no. 12, pp. 3160–3163, 1998.

[46] X. Chen, S. Cao, X. Weng, H. Wang, and Z. Wu, "Effects of morphology and structure of titanate supports on the performance of ceria in selective catalytic reduction of NO," *Catalysis Communications*, vol. 26, pp. 178–182, 2012.

[47] B. K. Vijayan, N. M. Dimitrijevic, J. Wu, and K. A. Gray, "The effects of Pt doping on the structure and visible light photoactivity of titania nanotubes," *Journal of Physical Chemistry C*, vol. 114, no. 49, pp. 21262–21269, 2010.

[48] Z. Tang, F. Li, Y. Zhang, X. Fu, and Y. J. Xu, "Composites of titanate nanotube and carbon nanotube as photocatalyst with high mineralization ratio for gas-phase degradation of volatile aromatic pollutant," *Journal of Physical Chemistry C*, vol. 115, no. 16, pp. 7880–7886, 2011.

[49] R. Yuan, B. Zhou, D. Hua, and C. Shi, "Enhanced photocatalytic degradation of humic acids using Al and Fe co-doped TiO_2 nanotubes under UV/ozonation for drinking water purification," *Journal of Hazardous Materials*, vol. 262, pp. 527–538, 2013.

[50] J. Kang, D. Aasi, and Y. Katayama, "Bisphenol A in the aquatic environment and its endocrine-disruptive effects on aquatic organisms," *Critical Reviews in Toxicology*, vol. 37, no. 7, pp. 607–625, 2007.

[51] T. Zhang, X. W. Zhang, X. L. Yan, J. W. Ng, Y. J. Wang, and D. D. Sun, "Removal of bisphenol A via a hybrid process combining oxidation on β-MnO_2 nanowires with microfiltration," *Colloids and Surfaces A: Physicochemical and Engineering Aspects*, vol. 392, no. 1, pp. 198–204, 2011.

[52] R. A. Doong, S. M. Chang, and C. W. Tsai, "Enhanced photoactivity of Cu-deposited titanate nanotubes for removal of bisphenol A," *Applied Catalysis B*, vol. 129, pp. 48–55, 2013.

[53] K. Lin, W. Liu, and J. Gan, "Oxidative removal of bisphenol A by manganese dioxide: efficacy, products, and pathways," *Environmental Science and Technology*, vol. 43, no. 10, pp. 3860–3864, 2009.

[54] Y. Y. Chen, S. M. Zhang, Y. Yu et al., "Synthesis, characterization, and photocatalytic activity of N–doped TiO_2 nanotubes," *Journal of Dispersion Science and Technology*, vol. 29, no. 2, pp. 245–249, 2008.

[55] H. Tokudome and M. Miyauchi, "N-doped TiO_2 nanotube with visible light activity," *Chemistry Letters*, vol. 33, no. 9, pp. 1108–1109, 2004.

[56] J. C. Xu, M. Lu, X. Y. Guo, and H. L. Li, "Zinc ions surface-doped titanium dioxide nanotubes and its photocatalysis activity for degradation of methyl orange in water," *Journal of Molecular Catalysis A: Chemical*, vol. 226, pp. 123–127, 2005.

[57] M. Pirilä, R. Lenkkeri, W. M. Goldmann, K. Kordás, M. Huuhtanen, and R. L. Keiski, "Photocatalytic degradation of butanol in aqueous solutions by TiO_2 nanofibers," *Topics in Catalysis*, vol. 56, no. 9-10, pp. 630–636, 2013.

[58] J. Kirchnerova, M.-L. Herrera Cohen, C. Guy, and D. Klvana, "Photocatalytic oxidation of *n*-butanol under fluorescent visible light lamp over commercial TiO_2 (Hombicat UV100 and Degussa P25)," *Applied Catalysis A: General*, vol. 282, no. 1-2, pp. 321–332, 2005.

[59] L. Song, J. Xiong, Q. Jiang, P. Du, H. Cao, and X. Shao, "Synthesis and photocatalytic properties of Zn^{2+} doped anatase TiO_2 nanofibers," *Materials Chemistry and Physics*, vol. 14, no. 1, pp. 77–81, 2013.

[60] L. Qin, X. Pan, L. Wang, X. Sun, G. Zhang, and X. Guo, "Facile preparation of mesoporous TiO_2(B) nanowires with well-dispersed Fe_2O_3 nanoparticles and their photochemical catalytic behavior," *Applied Catalysis B: Environmental*, vol. 150-151, pp. 544–553, 2014.

[61] M. A. Fontecha-Cámaraa, M. A. Álvarez-Merinoa, F. Carrasco-Marínb, M. V. López-Ramóna, and C. Moreno-Castillab, "Heterogeneous and homogeneous Fenton processes using activated carbon for the removal of the herbicide amitrole from water," *Applied Catalysis B: Environmental*, vol. 101, pp. 425–430, 2011.

[62] B. Liu, A. Khare, and E. S. Aydil, "TiO_2-B/anatase core-shell heterojunction nanowires for photocatalysis," *ACS Applied Materials and Interfaces*, vol. 3, no. 11, pp. 4444–4450, 2011.

[63] S. Ramasundaram, H. N. Yoo, K. G. Song, J. Lee, K. J. Choi, and S. W. Hong, "Titanium dioxide nanofibers integrated stainless steel filter for photocatalytic degradation of pharmaceutical compounds," *Journal of Hazardous Materials*, vol. 258-259, pp. 124–132, 2013.

[64] X. W. Zhang, T. Zhang, J. Ng, and D. D. Sun, "High-performance multifunctional TiO_2 nanowire ultrafiltration membrane with a hierarchical layer structure for water treatment," *Advanced Functional Materials*, vol. 19, pp. 3731–3736, 2009.

[65] A. Hu, X. Zhang, K. D. Oakes, P. Peng, Y. N. Zhou, and M. R. Servos, "Hydrothermal growth of free standing TiO_2 nanowire membranes for photocatalytic degradation of pharmaceuticals," *Journal of Hazardous Materials*, vol. 189, no. 1-2, pp. 278–285, 2011.

[66] X. W. Zhang, A. J. Du, P. Lee, D. D. Sun, and J. O. Leckie, "TiO_2 nanowire membrane for concurrent filtration and photocatalytic oxidation of humic acid in water," *Journal of Membrane Science*, vol. 313, no. 1-2, pp. 44–51, 2008.

[67] Z. L. He, W. X. Que, J. Chen, X. T. Yin, Y. C. He, and J. B. Ren, "Photocatalytic degradation of methyl orange over nitrogen-fluorine codoped TiO_2 nanobelts prepared by solvothermal synthesis," *ACS Applied Materials & Interfaces*, vol. 4, pp. 6815–6825, 2012.

[68] N. T. Q. Hoa, Z. Lee, S. H. Kang, V. Radmilovic, and E. T. Kim, "Synthesis and ferromagnetism of Co-doped TiO(2-delta) nanobelts by metallorganic chemical vapor deposition," *Applied Physics Letters*, vol. 92, no. 12, 2008.

[69] P. Gao, D. Bao, Y. Wang et al., "Epitaxial growth route to crystalline TiO_2 nanobelts with optimizable electrochemical performance," *ACS Applied Materials & Interfaces*, vol. 2, pp. 368–373, 2013.

[70] J. Lin, J. Shen, T. Wang et al., "Enhancement of photocatalytic properties of TiO_2 nanobelts through surface-coarsening and

surface nanoheterostructure construction," *Materials Science and Engineering B*, vol. 176, pp. 921–925, 2011.

[71] J. Zhang, W. Liu, X. Wang, B. Hu, and H. Liu, "Enhanced decoloration activity by Cu_2O@TiO_2 nanobelts heterostructures via a strong adsorption-weak photodegradation process," *Applied Surface Science*, vol. 282, pp. 84–91, 2013.

[72] J. Tian, Y. Sang, Z. Zhao et al., "Enhanced photocatalytic performances of CeO_2/TiO_2 nanobelt heterostructures," *Small*, vol. 9, no. 2, pp. 3864–3872, 2013.

[73] R. Liang, A. Hu, W. J. Li, and Y. N. Zhou, "A chemical approach to accurately characterize the coverage rate of gold nanoparticles," *Journal of Nanoparticle Research*, vol. 15, p. 1900, 2013.

[74] M. A. Khan, H. Jung, and O. B. Yang, "Synthesis and characterization of ultrahigh crystalline TiO_2 nanotubes," *Journal of Physical Chemistry B*, vol. 110, no. 13, pp. 6626–6630, 2006.

[75] L. Li, X. Qin, G. Wang, L. Qi, G. Du, and Z. Hu, "Synthesis of anatase TiO_2 nanowires by modifying TiO_2 nanoparticles using the microwave heating method," *Applied Surface Science*, vol. 257, no. 18, pp. 8006–8012, 2011.

[76] J. Lee, Y. Lee, H. Song, D. Jang, and Y. Choa, "Synthesis and characterization of TiO_2 nanowires with controlled porosity and microstructure using electrospinning method," *Current Applied Physics*, vol. 11, no. 1, pp. S210–S214, 2011.